Blocking Endocytosis Enhances Short-Term Synaptic Depression under Conditions of Normal Availability of Vesicles

Yunfeng Hua, Andrew Woehler, Martin Kahms, Volker Haucke, Erwin Neher, and Jürgen Klingauf
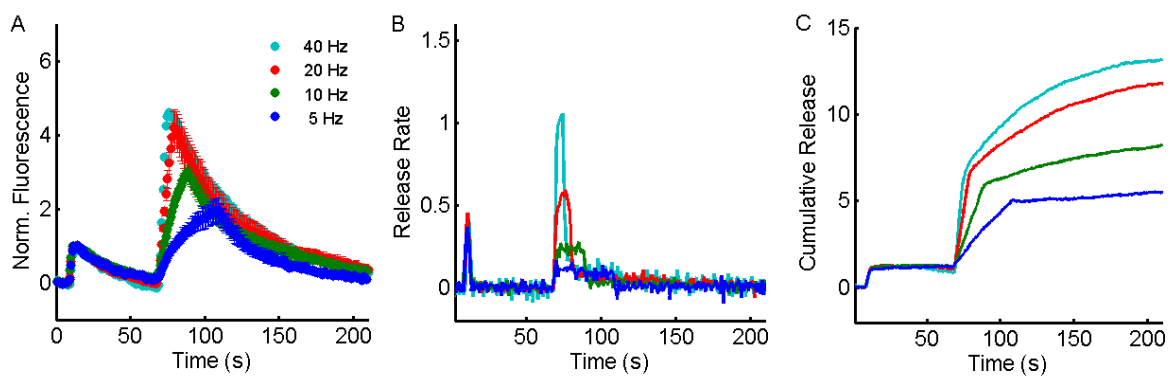

Figure S1. Endocytosis slows down after strong stimulation. Related to Figure 1.

(A) Average spH responses to 50 APs at 20 Hz followed by 200 APs at 5 Hz (blue, n = 6), 10 Hz (green, n = 3), 20 Hz (red, n = 3) or 40 Hz (cyan, n = 6). Between stimuli an interval of 60 sec was allowed for recovery. Fluorescence transients were normalized to the response amplitude of the calibration stimulus. Error bars represent s.e.m.

(B) Time courses of release rate calculated from (A) by deconvolution.

(C) Time courses of cumulative release calculated from (B). Integrating the release rate time course provided a estimation of cumulative release for quantitative comparison. An Increase of the endocytic rate constant upon strong stimulation leads to a misinterpretation, resulting in an increased amplitude of release and an apparent sustained release after stimulation.
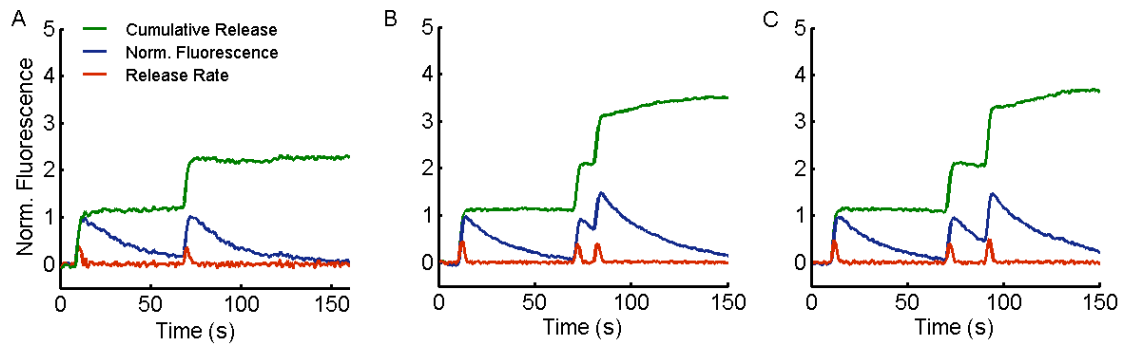
Figure S2. Validation of the deconvolution method. Related to Figures 1 and 3.

(A) Representative spH response to two identical stimulations (50 APs at 20 Hz for each, a similar release kinetics is expected during both stimulations), in between of which a 60 sec interval was given for recovery. Fluorescence transients were normalized to the amplitude of the calibration responses (blue, the blue trance is an average from 17 boutons). Deconvolution revealed two similar stimulation-locked peaks in the release rate time course (red). Integrating all release events over time provided a good estimation of the cumulative release (green). Two identical step increases were found for the two stimulation episodes, suggesting the same number of vesicles undergoing fusion.

(B) Like (A), however a third stimulation (50 AP @ 20 Hz) was given 10 sec after the second one. In the release rate time course (red) three release events could be clearly resolved despite the overlapping in the original fluorescence responses (blue), in which the third peak was superimposed on the decay phase of the second one. Cumulative release (green) revealed three identical step increases.

(C) The same experiment as in (B) , however the third stimulation was delivered 20 sec after the second one. Compared to (B), the amplitude of the third increase in cumulative release was not affected by prolonged interval (green). Taking together,

these experiments suggest that the outcome of deconvolution method serves as a good estimate for exocytosis.
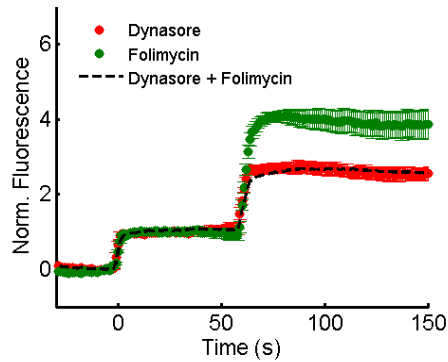

Figure S3. Reacidification has no effect on Dynasore induced release depression. Related to Figure 2.

Average spH responses to 50 APs at 20 Hz followed by 200 APs at 40 Hz in the presence of Dynasore (red, n = 6), Folimycin (green, n = 6) or both (black broken line, n = 3). Between stimuli a 60 s interval was given for recovery. Each fluorescence transient was normalized to the response amplitude of the calibration stimulus. In the presence of both Folimycin and Dynasore resulted in same signal amplitude compared to that of only using Dynasore and about 38 % smaller than that of using Folimycin. Error bars represent s.e.m.
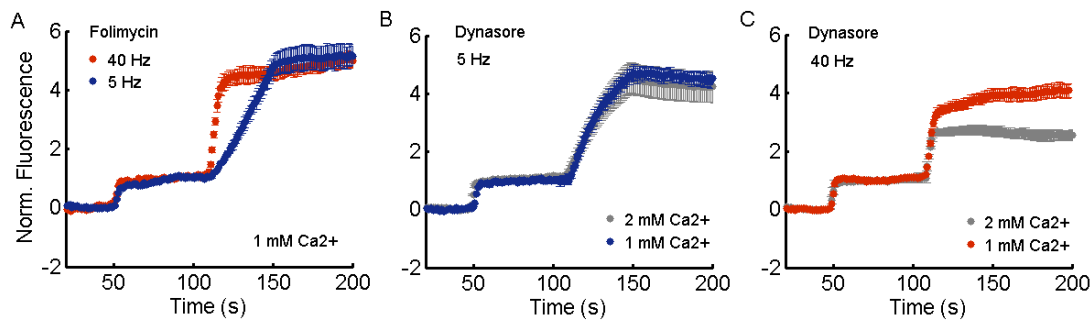
Figure S4. Decrease exocytosis leads to less release depression. Related to Figure 2.

(A) Average spH responses to 50 APs at 20 Hz followed by 200 APs at 5 (blue, n = 5) or 40 Hz (red, n = 5) in the presence of 80 nM Folimycin and 1 mM Calcium. Each fluorescence transient was normalized to the response amplitude of the calibration stimulus. Both 40 Hz and 5 Hz stimulation could evoke same amount of vesicle fusion. Error bars represent s.e.m.

(B) Average spH responses to 50 APs at 20 Hz followed by 200 APs at 5 Hz in the presence of 100 μM Dynasore and 1 mM Calcium (blue *n* = 6). For comparison, fluorescence transient from the same experiment performed in 2 mM Calcium is plotted (gray, from Fig 2 B). No difference was observed in normalized amplitude. Error bars represent s.e.m.

(C) Average spH responses to 50 APs at 20 Hz followed by 200 APs at 40 Hz in the presence of 100 μM Dynasore and 1 mM Calcium (red *n* = 6). An increase in normalized amplitude was observed compared with fluorescence transient from the same experiment performed in 2 mM Calcium (gray, from Fig 2 B). Error bars represent s.e.m.

Supplemental Experimental Procedures

Normalization and Deconvolution of SpH Signal

In previous studies (Burrone et al., 2006; Hua et al., 2010; Newton et al., 2006; Sankaranarayanan et al., 2000), the normalization of the fluorescence responses was performed either with respect to the SV pool size or simply with respect to the base-line fluorescence, neither of which correlates strongly to spH expression level and release probability of synapses. Therefore, even after such normalization large variation in amplitudes of response still remains, especially for small sample populations. Here, we made use of relatively constant spH expression levels and release probabilities of given synapses over short experimental time windows by using a paired-stimulation protocol, in which a calibration stimulus (50 APs at 20 Hz) was followed by a 60-second recovery interval and the test stimulus of interest. The calibration stimulus is believed to only trigger the fusion of docked vesicles (Murthy and Stevens, 1999; Schikorski and Stevens, 1997). Fluorescence transients resulting from the test stimuli and measured on individual boutons were normalized to the amplitudes of the corresponding calibration stimulation responses, providing a signal that is independent of release probability and spH expression level (Suppl. 1 A).

Deconvolution of SpH Signal

The vesicle retrieval time constant has been reported to be a cell-wide property and to remain constant upon multiple rounds of trials for individual cells (Armbruster and Ryan, 2011). Therefore, assuming that the measured signal is a linear sum of elementary events, the relative release rate may be calculated by deconvolution of the signal. In practice, we first extracted information about the kinetics of endocytosis and reacidification by fitting an exponential function to the decay phase of each calibration response. In order to minimize noise during

deconvolution, we took the obtained decay function instead of real data as a template. The deconvolution was then performed by forming the ratio between a given trace and template in Fourier space using a Matlab built-in function (Suppl. 1 B). However, whenever the cell was challenged with prolonged stimulation (about 200 APs and more) at 10 Hz or higher frequencies, deconvolution also seemed to indicate continued release after stimulation (Suppl. 1 C). In line with previous observations (Balaji et al., 2008), this effect was traced to an increased endocytic time constant under such condition. A potential explanation for the progressive decline in endocytic rate is that exocytosis-driven protein accumulation on the surface exceeds the buffering capacity of the readily retrievable surface pool for the fast endocytosis, as suggested in previous studies (Balaji et al., 2008; Hua et al., 2011). To determine the range of constancy of the endocytic time constant, which also defines the range of validity of deconvolution, we explored the relationship between the stimulation strength and the resulting endocytic time constant (Figure 1 D). We found that at low stimulation frequency (5 Hz) the endocytic time constant is relatively insensitive to increases in the total number of stimuli. Similarly at low total number of stimuli (50 APs) it is insensitive to increases in stimulation frequency. For a given stimulation frequency above 5 Hz, however (10, 20 or 40 Hz), the endocytic rate constant remains relatively stable only for a limited number of stimuli, beyond which the rate decreases rapidly. In the range of mild stimulation conditions, the recovery of the readily retrievable pool may be fast enough to cope with the exocytic load and thereby ensure maximum speed of endocytosis for prolonged stimulation. This result confirms the existence of a limited surface capacity for fast membrane retrieval from the readily retrievable pool and suggests that the repopulation of this pool might limit the rate of the endocytosis. For our propose, when the exocytic load does not exceed the buffering capacity of the readily retrievable pool, the endocytic rate constant is maximal and remains relatively invariant, ensuring reliability of the outcome from the deconvolution method for studying vesicle exocytosis (Suppl. 2).

Supplemental References

Armbruster, M., and Ryan, T.A. (2011). Synaptic vesicle retrieval time is a cell-wide rather than individual-synapse property. Nat Neurosci *14*, 824-826.

Balaji, J., Armbruster, M., and Ryan, T.A. (2008). Calcium control of endocytic capacity at a CNS synapse. J Neurosci *28*, 6742-6749.

Burrone, J., Li, Z., and Murthy, V.N. (2006). Studying vesicle cycling in presynaptic terminals using the genetically encoded probe synaptopHluorin. Nat Protoc *1*, 2970-2978.

Hua, Y., Sinha, R., Martineau, M., Kahms, M., and Klingauf, J. (2010). A common origin of synaptic vesicles undergoing evoked and spontaneous fusion. Nat Neurosci *13*, 1451-1453.

Hua, Y., Sinha, R., Thiel, C.S., Schmidt, R., Huve, J., Martens, H., Hell, S.W., Egner, A., and Klingauf, J. (2011). A readily retrievable pool of synaptic vesicles. Nat Neurosci *14*, 833-839.

Murthy, V.N., and Stevens, C.F. (1999). Reversal of synaptic vesicle docking at central synapses. Nat Neurosci *2*, 503-507.

Newton, A.J., Kirchhausen, T., and Murthy, V.N. (2006). Inhibition of dynamin completely blocks compensatory synaptic vesicle endocytosis. Proc Natl Acad Sci U S A *103*, 17955-17960.

Sankaranarayanan, S., De Angelis, D., Rothman, J.E., and Ryan, T.A. (2000). The use of pHluorins for optical measurements of presynaptic activity. Biophys J *79*, 2199-2208.

Schikorski, T., and Stevens, C.F. (1997). Quantitative ultrastructural analysis of hippocampal excitatory synapses. J Neurosci *17*, 5858-5867.